DOI:10.1021/jf9039364

JOURNAL OF AGRICULTURAL AND FOOD CHEMISTRY
ARTICLE

Adsorption Equilibria of Water Vapor on Cork

Sonia Lequin,[†,‡,§] David Chassagne,[†,‡] Thomas Karbowiak,[‡] Régis Gougeon,[†,‡] Laurent Brachais,[‡] and Jean-Pierre Bellat*[,§]

[†]Institut Universitaire de la Vigne et du Vin, Institut Jules Guyot, 1 Rue Claude Ladrey, Université de Bourgogne, F-21078 Dijon, France, [‡]EA 581 EMMA, Dijon Agrosup, 1 Esplanade Erasme, Université de Bourgogne, F-21078 Dijon, France, and [§]Laboratoire Interdisciplinaire Carnot de Bourgogne, ICB UMR 5209 CNRS, 9 Avenue Alain Savary, Université de Bourgogne, F-21078 Dijon, France

We report here for the first time a complete thermodynamic study of water vapor adsorption on crude cork powder and plate. Adsorption−desorption isotherms were accurately measured by thermogravimetry at 283, 298, and 313 K in a large range of relative pressure. Adsorption enthalpies were determined by calorimetry as a function of loading. Adsorption−desorption isotherms exhibit a hysteresis due to the swelling of the material. The influence of the presence of lenticels on the adsorption properties of cork is found to be negligible. A detailed analysis and interpretation of adsorption data allow proposal of an adsorption mechanism in two steps. (i) First, water adsorbs on hydrophilic sites constituted by hydroxyl and methoxyl groups. (ii) Then water adsorption continues by clusters formation around the hydrophilic sites.

KEYWORDS: Cork; water; adsorption; thermogravimetry; calorimetry; solid state NMR

INTRODUCTION

Cork, constituting the outer bark of oak tree *Querçus suber* L., is a natural and renewable material with peculiar mechanical, physical, and chemical properties. It reveals an alveolar and anisotropic structure without intercellular spaces (*1*−*3*) but with lenticular channels named lenticels. These lenticels constitute the main porosity of cork (*4*). The structure of cork cell wall is made up of three layers. The thin middle lamella or internal primary wall is composed of lignin. Lignin represents about 25% of the total material weight and offers the mechanical support and rigidity of cell walls. Without lignin cork cells would totally collapse. The thick secondary cell wall is made up of alternating suberin and wax lamella. Suberin, the main component of cork (about 50%), is a polyester whose structure is not yet well-known. It is composed of long chains of fatty acids, hydroxyl fatty acids, and phenolic acids linked by ester groups (*5*−*7*). Finally, a thin layer of celluloses and hemicelluloses with a proportion of about 10 wt % constitutes the tertiary wall.

Cork is known to be light, compressible, and impermeable to liquids and gases, allowing its use in a lot of application fields. Some of them have been known for a long time, such as thermal and vibration insulation, wall and floor covering, or cork object making (cigarette box, desk pads, mouse pad, mats, shoe soles, memo board, shuttlecocks, ...) (*8*). The main sector of cork industry remains the production of natural cork stoppers. Cork has been used since antiquity for sealing alcoholic beverages, particularly wines. However, production of cork stoppers really started during the 19th century with the development of the glass bottle industry. But cork will have to wait an additional century to give rise to a relevant interest in wine scientific research because of cork taint (*9*). More recently, different potential applications were discovered (therapeutic shoes (*10*), antiaging skin, medicine effects like tumor inhibition (*11*−*13*), ...). Another possible interesting use of cork is the biosorption of pollutants. Its good performances and low cost make it a good candidate for biosorption of heavy metals such as Cu(II), Zn(II), Cr(VI), and Ni(II) (*14*, *15*), pesticides (*16*), etc.

Cork and wood are very similar materials. The topochemistry of the cell wall is quite the same except for the secondary wall of wood which is constituted of cellulose. As for wood, physical properties of cork are strongly dependent on its water content. Surprisingly, if the interaction of water with wood has been largely studied (*17*−*24*), data relative to adsorption of water by cork are very scarce (*25*−*27*). To our knowledge, the only data reported in the literature are those of Abdulla et al. (*23*), Gonzales Adrados et al. (*24*), and Gil et al. (*25*) These authors measured the adsorption isotherms of water vapor on cork at several temperatures, modeled the adsorption isotherms, and estimated the isosteric adsorption heat. However, they did not study desorption and no accurate measurements are given for adsorption enthalpies and molar adsorbate entropies as a function of the adsorbed amount. Therefore, a more detailed study was necessary in order to acquire a better knowledge concerning the interactions of water with cork. The objective of this study was thus to perform a complete thermodynamic study of the adsorption of water vapor on cork. Adsorption and desorption were accurately studied, and a few explanations are put forward concerning the hysteresis phenomenon observed in desorption. Special attention was paid to the role of lenticels in water adsorption. Original solid state NMR experiments were also conducted to attempt the

*To whom correspondence should be addressed. Telephone: +33 (0) 3 80 39 59 29. Fax: +33 (0) 3 80 39 61 32. E-mail: jean-pierre.bellat@u-bourgogne.fr.

 Published on Web 03/01/2010

Table 1. Temperature of Adsorption, Water Vapor Pressure, and Relative Pressure Ranges Investigated by Thermogravimetry for Cork Plate and Cork Powder

cork sample	T, K	p range, hPa	p_s, hPa	p/p_s range
powder	313	0.4−20	73.6	0.005−0.27
plate and powder	298	0.5−30	31.5	0.0015−0.95
powder	283	0.2−10	12.1	0.017−0.90

identification of water adsorption sites. Results obtained in this work will be very useful for the development of different applications mentioned above, notably for those concerning wine which contains about 90% of water.

EXPERIMENTAL PROCEDURES

Material. Raw cork planks, from *Quercus suber* L. oak trees in the Mora (Portugal) production area, were supplied by Bouchons Trescases S.A. (Boulou, France). Planks were neither washed nor surface treated (with paraffin or silicone) prior to use. Uniform cork pieces in plate geometry, 35 mm long, 10 mm wide, and 1 mm thick for gravimetric study of water vapor adsorption, were manually cut from the planks. The matter present in the lenticels (lenticular cells) was extracted from the planks by scraping with a cutter blade. Cork powder, with and without lenticels, was also used. Powder is made by grating cork stopper or cork plate with a rasp. After sieving, the mean particle size was lower than 500 μm.

Thermogravimetry. Adsorption of water vapor on natural cork was investigated by thermogravimetry with a homemade McBain balance, under controlled temperature and pressure. The adsorption−desorption isotherm was measured step by step using a static method. Once a plateau of mass was recorded, the next equilibrium was reached by changing the water vapor pressure. Two samples with different geometries were studied: cork plate and cork powder. The mass of the cork sample was around 40 mg. Prior to each experiment, the cork sample was outgassed in situ under vacuum (10^{-5} hPa) at 298 K until a plateau of mass is reached. This needed 12 h for the powder and 24 h for the plate. After this treatment the water content did not exceed 1 wt %. The adsorption temperatures and the water vapor pressure ranges investigated for cork plate and cork powder are reported in **Table 1**. The corresponding ranges of relative pressure p/p_s, p_s being the saturation water vapor pressure at the adsorption temperature, are also indicated. The experimental accuracy is ± 0.01 mmol$\cdot$g^{-1} for the adsorbed amount, ± 0.5 K for the temperature, and ± 0.01 hPa for the pressure.

Differential Calorimetry Coupled with Manometry. Adsorption enthalpy of water vapor on cork was measured with a differential calorimeter (Thian-Calvet Setaram C80) coupled with manometry. This device has been described in detail in previous studies (*28*−*30*). It allows measuring the molar adsorption enthalpy $\Delta H^a(m^a)$ of water, so-called the adsorption heat, as a function of the adsorbed amount m^a. Adsorption was realized at 298 K on about 640 mg of cork powder, previously outgassed in situ under vacuum at 10^{-5} hPa for 72 h. The water vapor pressure ranged from 0.1 to 25 hPa.

High Resolution Solid State NMR. NMR experiments were carried out at 293 K on cork samples either outgassed under vacuum and kept under argon for analysis or previously equilibrated at 293 K under water relative pressures of 0.11 and 0.98 using lithium chloride and potassium dichromate saturated salt solution, respectively. These NMR experiments were run on a Bruker DSX 300 spectrometer operating at frequencies of 300.1 and 75.5 MHz for ^{1}H and ^{13}C, respectively. All spectra were acquired with a Bruker double-channel 4 mm MAS probe at 10 kHz spinning rate. The ^{1}H−^{13}C spectra were obtained by cross-polarization (CP-MAS), with spinal-64 proton dipolar decoupling. The experimental conditions were as follows: a ^{1}H 90° pulse of 3.6 μs, a contact time of 1 ms, and a recycle delay of 4 s between consecutive pulses. Hartmann−Hahn matching for the ^{1}H−^{13}C CP-MAS experiments was set on adamantane for ^{1}H and ^{13}C radiofrequency fields of ~60 kHz. Chemical shifts for ^{1}H and ^{13}C spectra were referenced to the signal of water (4.87 ppm) and to the methylene signal of adamantane (29.47 ppm), respectively.

Modeling of Adsorption Isotherms. The modeling of adsorption isotherms was performed by the well-known BET and GAB equations. Modeling was only performed on adsorption isotherms determined on cork powder at different temperatures. Mathematical equations of these models are briefly recalled below.

BET Model. The Brunauer, Emmet, and Teller (BET) model is well adapted to describe a mono- and multilayer gas adsorption in a relative pressure range between 0.05 and 0.4 (*31*). This model is defined by the following relation:

$$\frac{m^a}{m_m} = \frac{C(p/p_s)}{(1-p/p_s)[1+(C-1)(p/p_s)]} \quad (1)$$

where m^a is the full amount of adsorbed water (mmol$\cdot$g^{-1}), m_m is the amount of water adsorbed on the monolayer (mmol$\cdot$g^{-1}), p/p_s is the relative pressure, and C is a constant related to adsorption energies of the first and subsequent adsorbed layers. The adsorption energy of subsequent layers is assumed to be equal to the pure adsorptive liquefaction energy. C is related to the temperature by the relation

$$C_{BET} = C_{oBET}\, e^{-(\Delta H_{BET} - \Delta H_{liq})/(RT)} \quad (2)$$

where ΔH_{BET} is the adsorption enthalpy of the monolayer and ΔH_{liq} is the liquefaction enthalpy.

GAB Model. The Guggenheim−Anderson−de Boer (GAB) model is a refined extension of the BET theory (*32*). It is expressed as the following equation:

$$\frac{m^a}{m_m} = \frac{CK(p/p_s)}{[1-K(p/p_s)][1-K(p/p_s)+CK(p/p_s)]} \quad (3)$$

In this model, the properties of the subsequent layers are discriminated from those of the pure liquid bulk. The C constant is related to adsorption energies of the first and second layers, whereas the K constant is related to the adsorption energies of the second and subsequent layers which lie somewhere between the monolayer adsorption energy and the pure adsorptive liquefaction energy. These constants are defined by the relations (*33*)

$$C_{GAB} = C_{oGAB}\, e^{-(\Delta H_{GAB1} - \Delta H_{GABn})/(RT)} \quad (4)$$

$$K_{GAB} = C_{oGAB}\, e^{-(\Delta H_{GABn} - \Delta H_{liq})/(RT)} \quad (5)$$

where ΔH_{GAB1} is the adsorption enthalpy of the first layer and ΔH_{GABn} is that of the subsequent layers.

The GAB model was recently reconsidered by Pradas et al. (*34*) from thermodynamic and statistical mechanic statements. They showed that the GAB equation takes into account the possibility of an incomplete occupation of the first adsorption layer even at saturation. Thus, the GAB equation appears more appropriate to describe an adsorption process by clusters formation around localized adsorption sites rather than by formation of a homogeneous monolayer followed by multilayer condensation on the surface as considered in BET theory.

RESULTS AND DISCUSSION

Adsorption Isotherms. The adsorption−desorption isotherms of water vapor on plate and powder cork at 298 K are shown in **Figure 1**. Both curves display a type II shape of the IUPAC classification (*35*), typical of the adsorption on nonporous or macroporous solids.

The slope of adsorption isotherms, when the relative pressure tends to zero, is rather low. This indicates a weak adsorption affinity of water for cork. Indeed, the Henry constant given by this slope is about 5 and 10 mmol$\cdot$g^{-1} for plate and powder, respectively. These values are slightly higher than those reported for activated carbons (1−4 mmol$\cdot$g^{-1}), which are hydrophobic materials (*36*, *37*). However they are 10 times lower than those observed on silica gel (30−40 mmol$\cdot$g^{-1}), which is hydrophilic and often used as desiccant (*38*, *39*). Thus, cork can be considered as a rather hydrophobic material. This is in agreement with wettability measurements of water on crude cork, which showed

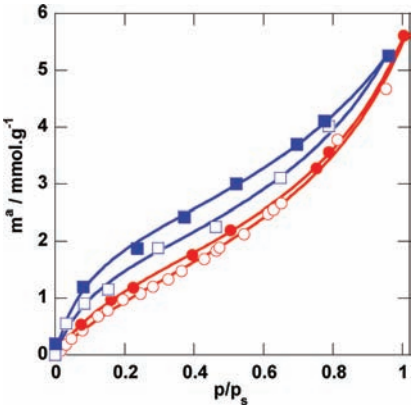

Figure 1. Adsorption−desorption isotherms of water vapor on dry cork plate (circles) and dry cork powder (squares) at 298 K: open symbols, adsorption; closed symbols, desorption.

that water is a nonwetting liquid for the cork surface (*40*). This hydrophobicity of the cork surface is attributed to the presence of suberin (*41*).

When the relative pressure is approaching 1, the adsorbed amount is around 6 mmol·g^{-1}. This corresponds to 11 wt %. This value is in good agreement with those found by other authors on cork granules of 0.5−1 mm (*25*) and on little pieces of cork (*26*). This adsorption capacity is rather low compared to microporous activated carbons or silica gels that can adsorb up to 40−50 wt %. It is nevertheless higher than that observed for very hydrophobic materials such as pure siliceous materials (2.2 mmol·g^{-1}) (*42*).

Adsorption isotherms on powder and on plate exhibit a hysteresis loop. The adsorption−desorption process is not reversible, especially on powder, for which the amplitude of the hysteresis is more noticeable. However, in both cases, desorption is total; no water remains adsorbed after pumping under vacuum. This means that no water molecule is chemically bonded to the surface. Water is only physisorbed. So the hysteresis phenomenon cannot be due to chemisorption. This kind of hysteresis has already been observed for water sorption on U.S. hardwoods, eucalyptus, pine, beech, spruce, and mahogany heartwood (*21*, *43*−*45*). Studies of water adsorption on lignin and cellulose, some of the major chemical components of wood, also reported the existence of a hysteresis loop in the adsorption−desorption isotherms (*46*, *47*). This hysteresis phenomenon is attributed to swelling effects that take place during hydration. In these lignocellulosic materials the adsorption mechanism is described in two steps (*19*). (i) First, water adsorbs on the surface, where it forms clusters around hydrophilic sites rather than a uniform monolayer. (ii) Then water diffuses into the cell wall. During this diffusion step, mechanical strengths occur between hydrated and dry layers, leading to a swelling of the material. This swelling depends on the water vapor pressure, the cell wall thickness, and the geometry of the sample (block or powder). In the case of cork, which is also a lignocellulosic material, the hysteresis phenomenon has certainly the same origin. Cork cell walls are probably hydrated with swelling effects as for wood.

It is noteworthy that adsorbed amounts are higher on cork powder than on cork plate, whatever the relative pressure. This difference could be attributed to the increase of the external surface area after grating. However, the difference in adsorbed amounts is not so important compared to the difference in the external surface between these two geometries (about 0.04 m^2·g^{-1} for the plate and about 163 m^2·g^{-1} for the powder). In another study, Nakano (*20*) also observed a slight difference between powder and block wood from Todomatsu (*A. sachalinensis* Fr. Schm.). He explained it by a more restricted swelling in block cork. Grating destroys the cell structure of wood by breaking bonds between microfibers. The material then becomes more elastic and consequently more sensitive to swelling during water adsorption. Since the amplitude of the hysteresis loop is higher in cork powder than in cork plates, a similar phenomenon in cork could be postulated. However, this increase in of the adsorption capacity of cork after grating might also be due to the creation of new hydrophilic sites by breaking chemical bonds.

Table 2. BET and GAB Parameters and Adsorption Enthalpies for Adsorption of Water Vapor on Cork Powder at Different Temperatures

p/p_s range of validity	T, K	m_m, mmol·g^{-1}	C	K	ΔH_{BET}, kJ·mol^{-1}	ΔH_{GAB1}, kJ·mol^{-1}	ΔH_{GABn}, kJ·mol^{-1}
			BET Model				
0−0.4	283	1.4	15.6		−60		
0−0.4	298	1.3	15.6		−60		
0−0.4	313	1.3	9.6		−60		
			GAB Model				
0−0.99	283	1.5	18.0	0.8		−75	−50
0−0.95	298	1.7	11.8	0.7		−75	−50
0−0.27	313	1.2	9.7	1.1		−75	−50

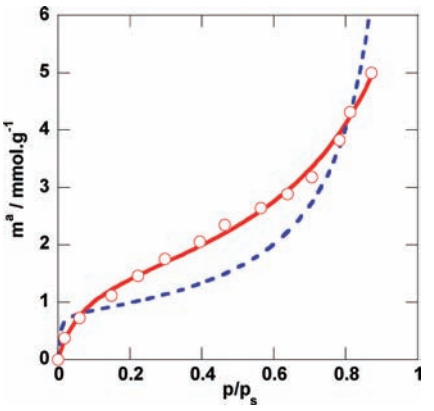

Figure 2. Modeling of adsorption isotherm of water vapor on dry cork at 283 K: (○) experiment; (- - -) BET model; (−) GAB model.

Modeling of Adsorption Isotherms. Values of BET and GAB parameters (m_m, C, and K) are collected in **Table 2**. The notion of monolayer is replaced below by that of "equivalent monolayer" because water molecules can form clusters on cork surface. The modeling of adsorption isotherms is shown in **Figure 2**. The best fit is obtained with the GAB model which gives a more accurate description of the adsorption process throughout the range of pressures explored.

The equivalent monolayer lies between 1.2 and 1.7 mmol·g^{-1} according to the temperature and the model used. This corresponds to 2.16 - 3 wt %. These values are in good agreement with those found in the literature on cork granules (*25*) (2.4 wt %) and cellulose (*48*) (3.3 wt %) at 298 K.

As expected, the value of the C constant decreases when the temperature increases. It is not the case for the K constant, the value of which is higher at 313 K than at lower temperatures. The value of K at this temperature is probably wrong, the range of relative pressure investigated being too much restricted to accurately determine this value.

Contribution of Matter Contained in Lenticels. Lenticels of cork are described as quasi-cylindrical channels composed of died cell walls and intercellular spaces. They cross cork along the radial direction without structural arrangement (**Figure 3**). Their

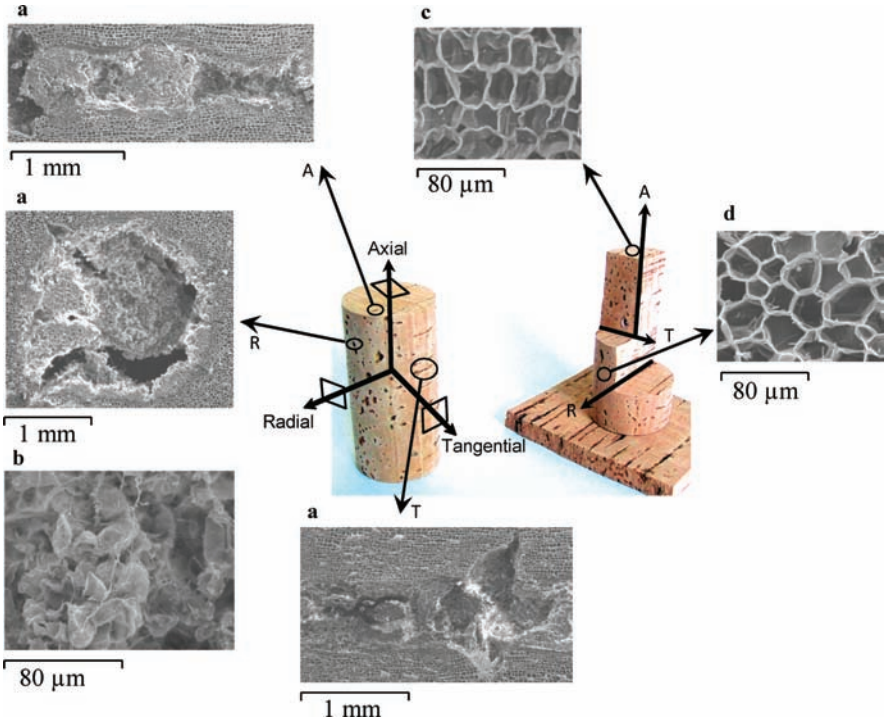

Figure 3. Scanning electronic microscopy pictures of (**a**) lenticels in axial (A), radial (R), and tangential (T) sections of cork, (**b**) the inside of lenticels, (**c**) cork cell in axial section, and (**d**) cork cell in radial section.

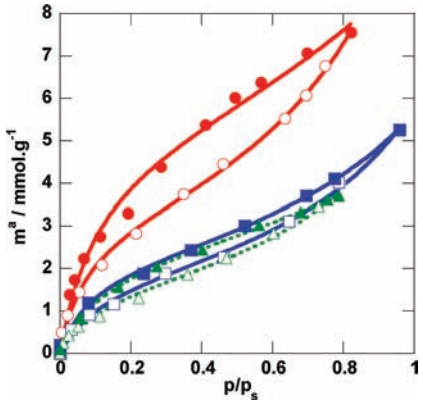

Figure 4. Adsorption−desorption isotherms of water vapor on lenticels (circles), dry cork powder without lenticels (squares), and dry cork powder with lenticels (triangles) at 298 K: open symbols, adsorption; closed symbols, desorption.

diameter is a few millimeters, and their length can reach several centimeters, depending on the cork thickness. They allow gas exchange between tree core and outside environment (*49*). The chemical composition of lenticular cells is close to that of wood cell wall. Lenticular cells are mainly constituted of lignin (about 47 wt %), polysaccharides (about 21 wt %), and extractives, mainly polar extractives (about 32 wt %) (*50*). Lenticels are overgrown by microorganisms (**Figure 3**, lower left-hand SEM picture). Lenticels create the macroporosity of cork. The ratio of lenticels in cork is used as the main indicator of cork quality in industrial applications (*3*). Therefore, it is of relevant interest to know if the lenticular cells play an important role in the adsorption process of water on cork.

Adsorption−desorption isotherms of water vapor on matter present in lenticels at 298 K are displayed in **Figure 4**. Those acquired for cork powder with and without lenticels are also reported for comparison. Adsorption−desorption isotherms of water vapor on lenticular cells have the same shape as those for cork. It similarly exhibits a hysteresis loop that is, however, more pronounced. The adsorbed amounts are higher than those measured for cork. At low relative pressures, the Henry constant (28 mmol·g^{-1}) and the C_{GAB} constant (18.6) are higher than those for cork. This indicates that the interactions with water are stronger in the case of lenticular cells. The value of the equivalent monolayer determined from GAB model (3.2 mmol·g^{-1}) is twice higher than for cork (1.7 mmol·g^{-1}). Likewise, the adsorption capacity close to saturation reaches 8 mmol·g^{-1} versus 6 mmol·g^{-1} for cork. These results show that lenticular cells are more hydrophilic than cork. Despite this, no noticeable difference in water vapor adsorption capacities is observed between powder with and without lenticels (**Figure 4**). This can be explained by the low lenticels content in this superior quality cork.

Adsorption Enthalpies and Entropies. Calorimetric adsorption enthalpies of water vapor on cork powder containing lenticels are given in absolute value versus loading in **Figure 5**. The values of adsorption enthalpies of the first and subsequent layers were also calculated from eqs **4** and **5** by plotting ln(constant) versus $1/T$. They are reported in **Table 2**.

When loading tends to zero, the adsorption enthalpy tends to 65 kJ·mol^{-1}. This value is of the same order of magnitude as those previously given by the BET and GAB theories (**Table 2**). The net adsorption enthalpy at zero loading, which is the difference between adsorption and liquefaction enthalpies, is equal to 21 kJ·mol^{-1}. It is similar to the value given by Abdulla et al.(*25*), using the isosteric method. This indicates that cork−water interactions are rather strong compared to water−water interactions occurring in the liquid bulk. However, this interaction energy is close to those usually involved in physisorption. As the adsorbed amount increases, the adsorption enthalpy continuously decreases and tends to the liquefaction enthalpy of water for loading which lies between 1.5 and 2 mmol·g^{-1}. This loading is very close to the "equivalent monolayer" determined by

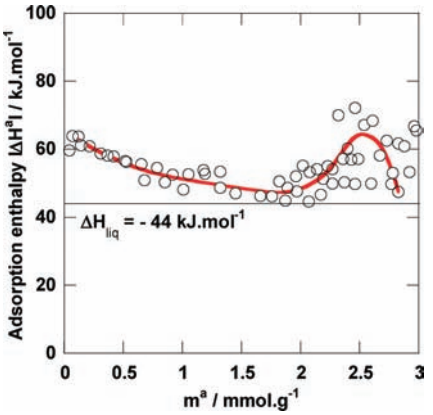

Figure 5. Adsorption enthalpy (absolute value) of water vapor on cork powder measured by calorimetry at 298 K versus loading. ΔH_{liq} is the liquefaction enthalpy of water.

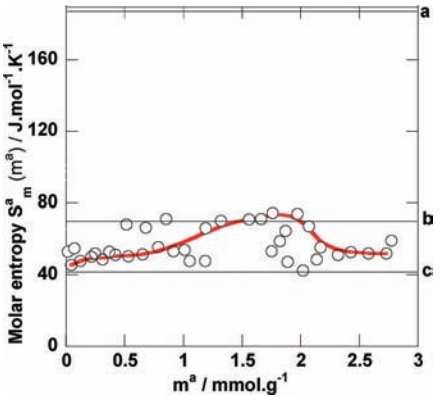

Figure 6. Molar entropy of water adsorbed on cork powder at 298 K as a function of loading: (**a**) standard molar entropy of gas $S_m^{g°}$ = 188.84 J·mol^{-1}·K^{-1}; (**b**) standard molar entropy of liquid $S_m^{l°}$ = 69.95 J·mol^{-1}·K^{-1}; (**c**) standard molar entropy of solid $S_m^{s°}$ = 41.50 J·mol^{-1}·K^{-1}.

BET and GAB models (**Table 2**). This first part of the calorimetric curve corresponds to the adsorption of water molecules on hydrophilic sites. The first molecules are adsorbed on the more energetic sites and the following ones on sites of decreasing energy. The fact that the adsorption enthalpy decreases in this region suggests that the adsorbate−adsorbent interactions decrease and that the adsorbate−adsorbate interactions are negligible. In other words, at low loading, the adsorbed molecules are too far from each other to allow molecular interactions.

At loading higher than 2 mmol·g^{-1}, the adsorption enthalpy sharply increases up to about 70 kJ·mol^{-1} and then tends back to the liquefaction enthalpy of liquid bulk as expected when approaching saturation. This exothermic effect shows the emergence of strong molecular interactions in the adsorbed phase. This phenomenon could be caused by the aggregation of water molecules around the hydrophilic sites. The presence of this exothermic peak at high loading reinforces the hypothesis that the adsorption process occurs by formation of water clusters as advanced by Hartley et al.(*19*) for wood. We think that it cannot take place as a monolayer and multilayer condensation mechanism because in this case the adsorption enthalpy should remain close to the liquefaction enthalpy of water after completion of the monolayer, i.e., for loading above 2 mmol·g^{-1}.

The molar entropy of the adsorbed phase is calculated from adsorption isotherm and calorimetric data by using the following equation derived from the Clapeyron relation (*51*):

$$S_m^a(m^a) = \Delta H^a(m^a)/T - R\ln(p/p^\circ)_{m^a} + S_m^{g^\circ} \qquad (6)$$

where $S_m^{g^\circ}$ is the standard molar entropy of water vapor at 298 K and p° the standard pressure (10^5 Pa).

The evolution of the molar entropy of water adsorbed on cork powder as a function of loading at 298 K is shown in **Figure 6**. Standard molar entropy values for gas, liquid, and solid water at 298 K are also reported.

At low loading, the molar entropy of the adsorbate is close to that of the solid. This means that the first water molecules adsorbed on the strongest hydrophilic sites lose degrees of freedom. They are "frozen" on their adsorption sites and are in a solid-like physical state. As loading increases, the molar entropy increases to the molar entropy of liquid bulk. Water molecules are progressively adsorbed on less energetic sites and are more mobile. Then above 2 mmol·g^{-1}, a decrease in the molar entropy which gets closer to the molar entropy of the solid is observed. This sudden decrease of the molar entropy at high loading is attributed to the formation of clusters around the hydrophilic sites which are more structured than the liquid bulk.

Molecular Investigation of Water Adsorption. In order to better characterize the possible adsorption sites and the interactions that can occur between the cork surface and water vapor, high resolution solid state ^{13}C NMR as a selective technique for a molecular scale investigation was used. **Figure 7** shows the ^{1}H−^{13}C (CP-MAS) NMR spectra of partially hydrated cork (pre-equilibrated under the relative pressure of 0.11) and completely hydrated cork (pre-equilibrated under the relative pressure of 0.98). From the literature on NMR of cork (*15*, *52*−*55*), most of the distinct peaks of cork can be identified. In particular, the low frequency peak at 30.1 and 32.9 ppm can be attributed to the carbon of the aliphatic methylene region of suberin (*15*, *52*−*54*). As no water molecule is assumed to bind to this chemical function, these two most intense and well-defined peaks unambiguously attributed to $-(CH_2)_n-$ of suberin were arbitrarily chosen to normalize the relative intensity of both spectra. The peak at 21.3 ppm can be assigned to the acetate function of hemicellulose (*53*, *54*). The peak at 56.2 ppm corresponds to the methoxy group from both lignin and suberin and also a small contribution from hemicellulose (*15*, *52*−*54*). The peak at 64.4 ppm can be tentatively attributed to the carbon number 6 of the carbohydrate unit from cellulose (*53*). The two peaks at 72.3 and 74.6 ppm are attributed to the carbons 2, 3, and 5 of the carbohydrate structure from cellulose, hemicellulose, and partly to side chain C−OH groups of lignin (*53*, *54*). The peaks at 82.4, 105.1, 130.1, and 173 ppm correspond respectively to the carbon 4 of the carbohydrate that could be attached to suberin, the anomeric carbon number of the carbohydrate that could also be attached to suberin, the aromatic carbons of suberin and lignin, and the carbonyl groups from suberin, hemicellulose, and lignin (ester groups and uronic acids) (*53*, *54*). The region of the spectrum between 62 and 105 ppm therefore contains overlapping signals from the three major constituents of cork.

Although not all the peaks can be unambiguously attributed, it is possible to draw information on the interactions between water and cork by comparing the relative intensity of a given ^{13}C peak of cork at low or high water loading (**Figure 7**). From adsorption data given in **Figure 1**, the 0.11 relative water pressure almost corresponds to the equivalent monolayer, whereas 0.98 lies near the saturation. The formation of clusters therefore occurs between these two limits from aggregation of water molecules around the hydrophilic sites already occupied.

If we compare the spectrum of partially hydrated cork (in orange) and that of completely hydrated cork (in blue), we can see

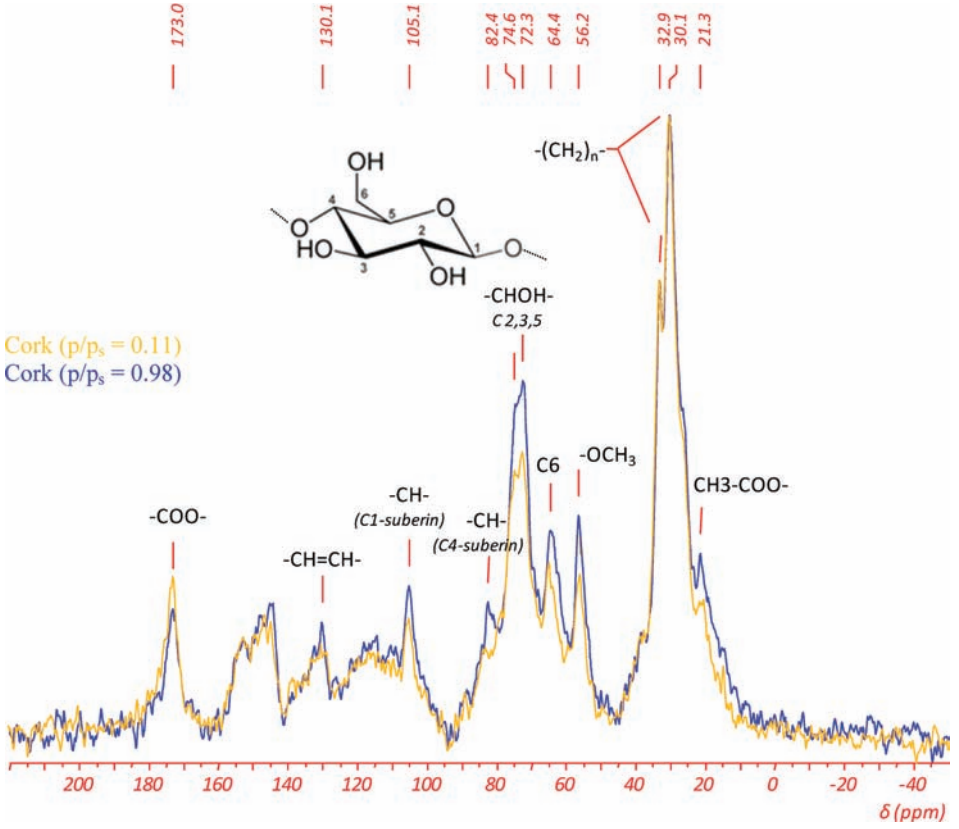

Figure 7. $^{1}H-^{13}C$ CPMAS spectrum of partially hydrated cork in orange (pre-equilibrated at water relative pressure of 0.11) and of completely hydrated cork (pre-equilibrated at water relative pressure 0.98) in blue. Spectra were obtained with a contact time of 1 ms and 1200 scans (p/p_s = 0.98) and 3700 scans (p/p_s = 0.11).

that the relative intensities of the peaks at 56.2, 64.4, 72.3, and 74.6 ppm are increased when water loading increases. The only factor that could induce such an increase is a better efficiency of the cross-polarization from nearby protons. Such a better efficiency can result from a reduced mobility of these nearby protons and/or from an increased density of nearby protons. In the present situation, additional protons would necessarily come from additional bound water molecules in the vicinity of these specific carbon sites. The water proportion introduced in the system increases from 0.55 to 5.3 mmol·g^{-1} for relative pressures from 0.11 to 0.98, respectively, as displayed by the adsorption isotherm in **Figure 1**. This suggests that water interacts specifically with some of the carbon sites offered by the cork structure. The four identified carbon sites that could be implied in the sorption process for water display attached chemical functions such as hydroxyl or methoxyl that can easily involve hydrogen bonds with water molecules. As the chemical structure and spatial distribution of cork constituents remain unknown, the location of the particular adsorption sites cannot be unambiguously identified. However, these results support the hypothesis of a specific physicochemical interaction in which the cellulosic fraction seems to play a significant contribution in the water sorption process.

Adsorption Mechanism of Water on Cork. This complete thermodynamics study and the detailed characterization of adsorbed water by NMR show that the adsorption of water on cork does not follow a monolayer and multilayer condensation process, as it could be expected considering the type II adsorption isotherm. It rather occurs according to a localized adsorption mechanism with aggregation of water molecules, as already emphasized for wood. First, water molecules are adsorbed on hydrophilic sites identified as hydroxyl or methoxyl groups that can easily involve hydrogen bonds with water molecules. Then the adsorption continues by formation of water clusters around the hydrophilic sites.

ABBREVIATIONS USED

C_{BET}, constant in BET equation; C_{GAB}, constant in GAB equation; C_{oBET}, Arrhenius type constant to express temperature dependence of C_{BET}; C_{oGAB}, Arrhenius type constant to express temperature dependence of C_{GAB}; K, constant in GAB equation; m, amount adsorbed (mmol·g^{-1}); m_m, amount of water adsorbed in the monolayer (mmol·g^{-1}); p, pressure (hPa); p_s, saturation water vapor pressure (hPa); $p°$, standard pressure (Pa); $S^a_m(m^a)$, molar entropy of the adsorbed phase; $S^{g°}_m$, standard molar entropy of water vapor at 298 K (J·mol^{-1}·K^{-1}); $S^{l°}_m$, standard molar entropy of liquid water at 298 K (J·mol^{-1}·K^{-1}); $S^{s°}_m$, standard molar entropy of solid water at 298 K (J·mol^{-1}·K^{-1}); T, temperature (K); amount adsorbed wt (%); $\Delta H^a(m^a)$, molar adsorption enthalpy at the loading m^a (kJ·mol^{-1}); ΔH_{BET}, adsorption enthalpy of the monolayer (kJ·mol^{-1}); ΔH_{GAB1}, adsorption enthalpy of the first layer (kJ·mol^{-1}); ΔH_{GABn}, adsorption enthalpy of the subsequent layers (kJ·mol^{-1}); ΔH_{liq}, liquefaction enthalpy (kJ·mol^{-1}).

ACKNOWLEDGMENT

We thank Christian Paulin, from Laboratoire Interdisciplinaire Carnot de Bourgogne (Dijon), for assistance regarding experimental techniques. We also thank Jésus Raya and Jérôme Hirschinger from the Laboratoire de Résonance Magnétique et de Biophysique des Membranes at University of Strasbourg for accessing the NMR spectrometer.

LITERATURE CITED

(1) Lequin, S.; Karbowiak, T.; Brachais, L.; Chassagne, D.; Bellat, J. P. Adsorption equilibria of sulphur dioxide on cork. *Am. J. Enol. Viticult*. **2009**, *60* (2), 138–144.

(2) Gibson, L. J.; Easterling, K. E.; Ashby, M. F. The structure and mechanics of cork. *Proc. R. Soc. London, Ser. A* **1981**, *377*, 99–117.

(3) Silva, S. P.; Sabino, M. A.; Fernandes, E. M.; Correlo, V. M.; Boesel, L. F.; Reis, R. L. Cork: properties, capabilities and applications. *Int. Mater. Rev*. **2005**, *50*, 345–365.

(4) Pereira, H. The Formation and Growth of Cork. In *Cork*; Elsevier Science B.V.: Amsterdam, 2007; pp 7−31.

(5) Gandini, A.; Pascoal Neto, C.; Silvestre, A. J. D. Suberin: a promising renewable resource for novel macromolecular materials. *Prog. Polym. Sci*. **2006**, *31* (10), 878–892.

(6) Graca, J.; Santos, S. Linear aliphatic dimeric esters from cork suberin. *Biomacromolecules* **2006**, *7* (6), 2003–2010.

(7) Cordeiro, N.; Belgacem, M. N.; Silvestre, A. J. D.; Pascoal Neto, C.; Gandini, A. Cork suberin as a new source of chemicals: 1. Isolation and chemical characterization of its composition. *Int. J. Biol. Macromol*. **1998**, *22* (2), 71–80.

(8) Pereira, H. Cork Products and Uses. In *Cork*; Elsevier Science B.V.: Amsterdam, 2007; pp 243−261.

(9) Buser, H. R.; Zanier, C.; Tanner, H. Identification of 2,4,6-trichloroanisole as a potent compound causing cork taint in wine. *J. Agric. Food. Chem*. **1982**, *30* (2), 359–362.

(10) Reiber, G. E.; Smith, D. G.; Wallace, C.; Sullivan, K.; Hayes, S.; Vath, C.; Maciejewski, M. L.; Yu, O.; Heagerty, P. J.; LeMaster, J. Effect of therapeutic footwear on foot reulceration in patients with diabetes: a randomized controlled trial. *JAMA, J. Am. Med. Assoc*. **2002**, *287* (19), 2552–2558.

(11) Moiteiro, C.; Marcelo Curto, M. J.; Mohamed, N.; Bailen, M.; Martinez-Diaz, R.; Gonzalez-Coloma, A. Biovalorization of friedelane triterpenes derived from cork processing industry byproducts. *J. Agric. Food. Chem*. **2006**, *54* (10), 3566–3571.

(12) Moiteiro, C.; Manta, C.; Justino, F.; Tavares, R.; Curto, M. J. M.; Pedro, M.; Nascimento, M. S. J.; Pinto, M. Hemisynthetic secofriedelane triterpenes with inhibitory activity against the growth of human tumor cell lines in vitro. *J. Nat. Prod*. **2004**, *67* (7), 1193–1196.

(13) Moiteiro, C.; Justino, F.; Tavares, R.; Marcelo-Curto, M. J.; Florencio, M. H.; Nascimento, M. S. J.; Pedro, M.; Cerqueira, F.; Pinto, M. M. M. Synthetic secofriedelane and friedelane derivatives as inhibitors of human lymphocyte proliferation and growth of human cancer cell lines in vitro. *J. Nat. Prod*. **2001**, *64* (10), 1273–1277.

(14) Chubar, N.; Carvalho, J. R.; Correia, M. J. N. Cork biomass as biosorbent for Cu(II), Zn(II) and Ni(II). *Colloids Surf., A* **2003**, *230* (1−3), 57–65.

(15) Villaescusa, I.; Fiol, N.; Cristiani, F.; Floris, C.; Lai, S.; Nurchi, V. M. Copper(II) and nickel(II) uptake from aqueous solutions by cork wastes: a NMR and potentiometric study. *Polyhedron* **2002**, *21* (14−15), 1363–1367.

(16) Domingues, V.; Alves, A.; Cabral, M.; Delerue-Matos, C. Sorption behaviour of bifenthrin on cork. *J. Chromatogr., A* **2005**, *1069* (1), 127–132.

(17) Barkas, W. W. Wood-water relationships, part III. Molecular sorption of water by sitka spruce wood. *Proc. Phys. Soc*. **1937**, *49* (3), 237–242.

(18) Spalt, H. A. Water-Vapor Sorption by Woods of High Extractive Content. *Proceedings: Wood Moisture Content, Temperature and Humidity Relationships*, Blacksburg, VA, October 29, 1979; Department of Agriculture, Forest Service: Washington, D.C., 1979; pp 55−61.

(19) Hartley, I. D.; Kamke, F. A.; Peemoeller, H. Cluster theory for water sorption in wood. *Wood Sci. Technol*. **1992**, *26* (2), 83–99.

(20) Nakano, T. Effects of cell structure on water sorption for wood. *Holzforschung* **2003**, *57* (2), 213–218.

(21) Okoh, K.; Skaar, C. Moisture sorption isotherms of the wood and inner bark of ten southern U.S. hardwoods. *Wood Fiber Sci*. **1980**, *12* (2), 98–111.

(22) Mandla, A. T.; Agnes, R. D.; Williams, R. S. Correlation of water vapor adsorption behavior of wood with surface thermodynamic properties. *J. Appl. Polym. Sci*. **1999**, *73* (3), 399–407.

(23) Rawat, S. P. S.; Khalid, D. P. Clustering of water molecules during adsorption of water in wood. *J. Polym. Sci., Polym. Phys*. **1998**, *36* (4), 665–671.

(24) Zhang, Y.; Zhang, S. Y.; Chui, Y. H. Water vapor adsorption and volumetric swelling of melt-impregnated wood-polymer composites. *J. Appl. Polym. Sci*. **2006**, *102* (3), 2668–2676.

(25) Abdulla, G.; Belghit, A.; Allaf, K. Impact of instant controlled pressure drop treatment on moisture adsorption isotherm of cork granules. *Drying Technol*. **2009**, *27* (2), 237–247.

(26) Adrados, J. R. G.; Haro, R. M. C. Variacion de la humedad de equilibrio del corcho en plancha con la humedad relativa. Modelos de regression no lineal para las isotermas de adsorcion. *Invest. Agrar., Sist. Recur. For*. **1994**, *3* (2), 199–209.

(27) Gil, L.; Cortiço, P. Cork hygroscopic equilibrium moisture content. *Holz Roh.- Werkst*. **1998**, *56*, 355–358.

(28) Moise, J.-C.; Bellat, J.-P. Effect of preadsorbed water on the adsorption of *p*-xylene and *m*-xylene mixtures on BaX and BaY zeolites. *J. Phys. Chem*. **2005**, *109* (36), 17239–17244.

(29) Weber, G.; Benoit, F.; Bellat, J.-P.; Paulin, C.; Mougin, P.; Thomas, M. Selective adsorption of ethyl mercaptan on NaX zeolite. *Microporous Mesoporous Mater*. **2008**, *109* (1−3), 184–192.

(30) Simonot-Grange, M. H.; Bertrand, O.; Pilverdier, E.; Bellat, J.-P.; Paulin, C. Differential calorimetric enthalpies of adsorption of *p*-xylene and *m*-xylene on y faujasites at 25°C. *J. Therm. Anal. Calorim*. **1997**, *48* (4), 741–754.

(31) Brunauer, S.; Emmett, P. H.; Teller, E. Adsorption of gases in multimolecular layers. *J. Am. Chem. Soc*. **1938**, *60* (2), 309–319.

(32) Anderson, R. B. Modifications of the Brunauer, Emmett and Teller equation. *J. Am. Chem. Soc*. **1946**, *68* (4), 686–691.

(33) Quirijns, E. J.; van Boxtel, A. J. B.; van Loon, W. K. P.; van Straten, G. Sorption isotherms, GAB parameters and isosteric heat of sorption. *J. Sci. Food. Agric*. **2005**, *85* (11), 1805–1814.

(34) Pradas, M. M.; Sanchez, M. S.; Ferrer, G. G.; Ribelles, J. L. G. Thermodynamics and statistical mechanics of multilayer adsorption. *J. Chem. Phys*. **2004**, *121* (17), 8524–8531.

(35) Sing, K. S. W.; Everett, D. H.; Haul, R. A. W.; Moscou, L.; Pierotti, R. A.; Rouquérol, J.; Siemieniewska, T. Reporting physisorption data for gas/solid systems. *Pure Appl. Chem*. **1985**, *57* (4), 603–619.

(36) Rutherford, S. W.; Coons, J. E. Equilibrium and kinetics of water adsorption in carbon molecular sieve: theory and experiment. *Langmuir* **2004**, *20*, 8681–8687.

(37) Qi, N.; LeVan, M. D. Adsorption equilibrium modeling for water on activated carbons. *Carbon* **2005**, *43* (11), 2258–2263.

(38) Ng, K. C.; Chua, H. T.; Chung, C. Y.; Loke, C. H.; Kashiwagi, T.; Akisawa, A.; Saha, B. B. Experimental investigation of the silica gel−water adsorption isotherm characteristics. *Appl. Therm. Eng*. **2001**, *21*, 1631–1642.

(39) Wang, X.; Zimmermann, W.; Ng, K.; Chakraboty, A.; Keller, J. Investigation on the isotherm of silica gel+water systems. *J. Therm. Anal. Calorim*. **2004**, *76* (2), 659–669.

(40) Gomes, C. M. C. P. S.; Fernandes, A. C.; de Almeida, B. d. J. V. S. The Surface tension of cork from contact angle measurements. *J. Colloid Interface Sci*. **1993**, *156* (1), 195–201.

(41) Cordeiro, N.; Pascoal Neto, C.; Gandini, A.; Belgacem, M. N. Characterization of the cork surface by inverse gas chromatography. *J. Colloid Interface Sci*. **1995**, *174* (1), 246–249.

(42) Flanigen, E. M.; Bennett, J. M.; Grose, R. W.; Cohen, J. P.; Patton, R. L.; Kirchner, R. M.; Smith, J. V. Silicalite, a new hydrophobic crystalline silica molecular sieve. *Nature* **1978**, *271*, 512–516.

(43) Christensen, G. N. Sorption and swelling within wood cell walls. *Nature* **1967**, *213* (5078), 782–784.

(44) Malmquist, L.; Söderström, O. Sorption equilibrium in relation to the spatial distribution of molecules. Application to sortpion of water by wood. *Holzforschung* **1996**, *50* (5), 437–448.

(45) Arévalo, R.; Hernandez, R. E. Influence of moisture sorption on swelling of mahogany (*Swietenia macrophylla* King) wood. *Holzforschung* **2001**, *55* (6), 590–594.

(46) Christensen, G. N.; Kelsey, K. E. The sorption of water vapour by the constituents of wood III. The swelling of lignin. *Aust. J. Appl. Sci*. **1959**, 30.

(47) Repellin, V.; Guyonnet, R. Evaluation of heat-treated wood swelling by differential scanning calorimetry in relation to chemical composition. *Holzforschung* **2005**, *59* (1), 28–34.
(48) Hollenbeck, G. R.; Peck, G. E.; Kildsig, D. O. Application of immersional calorimetry to investigation of solid−liquid interactions: Mmicrocrystalline cellulose−water system. *J. Pharm. Sci.* **1978**, *67* (11), 1599–1606.
(49) Groh, B.; Hübner, C.; Lendzian, K. Water and oxygen permeance of phellems isolated from trees: the role of waxes and lenticels. *Planta* **2002**, *215* (5), 794–801.
(50) Pereira, H. *Cork: Biology, Production and Uses*, 1st ed.; Elsevier: Amsterdam, 2007; p 336.
(51) Bellat, J.-P.; Simonot-Grange, M. H. Adsorption of gaseous *p*-xylene and *m*-xylene on NaY, KY and BaY zeolites. Part 2: Modeling. Enthalpies and entropies of adsorption. *Zeolites* **1995**, *15*, 219–227.
(52) Lopes, M. H.; Sarychev, A.; Pascoal Neto, C.; Gil, A. M. Spectral editing of ^{13}C CP/MAS NMR spectra of complex systems: application to the structural characterisation of cork cell walls. *Solid State Nucl. Magn. Reson.* **2000**, *16* (3), 109–121.
(53) Pascoal Neto, C.; Rocha, J.; Gil, A.; Cordeiro, N.; Esculcas, A. P.; Rocha, S.; Delgadillo, I.; De Jesus, J. D. P.; Correia, A. J. F. ^{13}C solid-state nuclear magnetic resonance and Fourier transform infrared studies of the thermal decomposition of cork. *Solid State Nucl. Magn. Reson.* **1995**, *4* (3), 143–151.
(54) Gil, A. M.; Lopes, M.; Rocha, J.; Pascoal Neto, C. A ^{13}C solid state nuclear magnetic resonance spectroscopic study of cork cell wall structure: the effect of suberin removal. *Int. J. Biol. Macromol.* **1997**, *20* (4), 293–305.
(55) Perra, B.; Haluk, J.-P.; Metche, M. IR, ^{1}H and ^{13}C NMR spectroscopic studies of suberin from beech bark (*Fagus sylvatica* L.). *Holzforschung* **1995**, *49*, 99–103.

Received for review November 12, 2009. Revised manuscript received February 10, 2010. Accepted February 15, 2010. We gratefully acknowledge the BIVB (Bureau Interprofessionnel des Vins de Bourgogne) and the Regional Council of Burgundy for financial support of this work (Project 2008-9201AAO024S00120), and the Trescases company for providing cork stoppers.